

Effects of honed cylinder surface topography on the wear of piston–piston ring–cylinder assemblies under artificially increased dustiness conditions

P. Pawlus

This paper presents results of the measurement of the surface roughness and other physical properties of the outer layer of honed cylinders. The cylinders tested had various surface topographies as a result of honing by abrasive tools of differing design. The results of wear measurements of the cylinders and piston rings mating with them during automotive gasoline Polonez 1500 engine operation under artificially increased dustiness conditions are presented and analysed.

Keywords: wear, abrasion, cylinder bores, cylinder surface, piston rings

Introduction

The piston–piston ring–cylinder assembly is the most important tribological system of an internal combustion engine. The surface finish of cylinder bores is one of the most significant factors affecting the compatibility of the sliding surfaces within the cylinder. Therefore in recent years the production of cylinder bores has received much attention from manufacturers. Honing is a typical technique used for cylinder finishing.

A survey of the literature reveals little information on the subject of the honed surface effect on co-acting parts wear in the case of high wear rates. An attempt is made in this paper to rectify this problem.

Kinds of wear of the piston–piston ring–cylinder assembly

The conditions of friction between a piston ring and a cylinder belong to the most difficult engine tribological assemblies. The most difficult conditions take place near the top dead centre (TDC) of the first piston ring. The high loads and temperatures and low relative velocity of the co-acting parts may be the reason for this. One can determine, based on analysis of the literature that in contemporary internal combustion engines near TDC of the first piston ring the oil film thickness amounts to 0–3 μm^1 . Low oil film thickness

is conducive to the existence of mitigated solid friction and semi-fluid friction between the piston ring and cylinder bearing surface². Fluid friction can exist in the middle part of the piston way. Contemporary investigators mention abrasive, corrosive and adhesive processes as predominant in this assembly^{3–8}. Some also include fatigue wear in this group^{2,9}. In References 10 and 11 the role of abrasive and adhesive wear is emphasized. However, the authors of References 1, 12 and 13 observe that abrasive and corrosive wear play significant roles in automotive internal combustion engines.

From the above literature survey one can conclude that the majority of research considers abrasion to be one of the predominant kinds of wear in piston–piston ring–cylinder assemblies. The process of abrasion comes into existence when incoherent or restrained abrasive particles are in the friction area. This kind of wear may be caused by rough jittings of a harder material which play the role of located microteeth. Abrasive wear in the presence of the abrasive material takes place when external debris as well as the products of wear penetrate between the sliding surfaces. Grinding particles from the air is the fundamental source of abrasive in the engine. Therefore finding a method which would allow intensifying abrasive wear of automotive engine cylinders as a consequence of supplying them with air polluted by quartz particles is a problem of unquestionable practical importance.

Rzeszów Technical University, Mechanical Engineering and Aviation Faculty, PO Box 85, 35-959 Rzeszów, Poland.

A survey of the literature on the influence of cylinder roughness topography on functional engine properties

Recommended specifications of leading engine builders with reference to honed cylinder surface roughness first of all include parameters obtained from the bearing length curve, connected with the profile height and describing the distribution and shape of the deep valleys^{3,14}.

Measurements of microhardness and residual stresses in the cylinder outer layer are carried out only during fundamental investigations. The majority of researchers think that cylinder surface microgeometry is the main factor affecting the operating conditions of the piston–piston ring–cylinder assembly, particularly in the running-in period.

At first, the recommended cylinder surface after honing was very smooth ($R_a = 0.2$). But considerable progress in engine construction caused a great scuffing inclination of the smooth cylinder surfaces. The results of Baumgarten¹⁵ and Wiemann¹⁶ show that the scuffing resistance of cylinders without additional surface treatment increases with an increase in their initial surface roughness.

For this reason Duck¹⁷ defines the recommended range of the parameter R_t for diesel engines as 4–7 μm , and for gasoline engines $R_t = 2.5 \mu\text{m}$. The authors of Reference 18 noticed a similar tendency based on the requirements of the leading engine builders. Differences among loads is the most probable reason for divergence among these requirements with respect to various types of engines. But an excessive growth of the cylinder surface roughness is also unprofitable as it causes increases in engine oil consumption¹⁷ as well as an increase in chromium piston ring wear¹⁹.

Therefore researchers made efforts to find a geometrical cylinder structure that might assure the sliding properties of smooth surfaces and a great ability to maintain oil on a porous surface. These requirements are best fulfilled by a plateau surface. It was found that a plateau surface assures shortening of running-in^{20–22}, lower wear in this period^{22,23} and an improvement in the selected engine operating parameters²².

It follows from analysis of the literature that cylinder surface topography affects engine properties in the initial period of engine life. However, some technical sources show that the influence of cylinder surface roughness on wear of piston–piston ring–cylinder assemblies may also exist in the case of large wear values.

The authors of References 4 and 19 found that lubricating oil and abrasive parts may accumulate in deep valleys. Sudarshan and Bhadun⁴ confirm that friction conditions become much worse after the valleys disappear. This means a possibility of a wear intensity increase from this moment. Barber and Ludema¹, presenting an analysis of the wear process of the cylinders of a Chevrolet engine, lead us to the same conclusion. Duck¹⁷ notes that honing valleys exist on the cylinder surface during long-term operation of the engine. It was found^{17,24} that, during engine use,

Table 1 Results of grain composition examination

Grain size range, μm	Mass fraction, %
0–2	15
2–5	13
5–10	16
10–20	21
20–40	23
> 40	12

settlement of microhardness course takes place, independently of its character after mechanical working. The shape of the microhardness distribution graph depends only on the conditions of cylinder wear (thermal conditions and deformation), which suggests that the physical properties of the cylinder outer layer may not influence its wear. Therefore the influence of cylinder surface topography on wear of piston–piston ring–cylinder assemblies is possible, particularly if the physical properties of their outer layers are similar.

Purpose and scope of the experiment

The fundamental aim of this work was to find a relation between cylinder roughness topography and wear of piston–piston ring–cylinder assemblies under artificially increased dustiness conditions.

Acceleration of the test was achieved by supplying air polluted by quartz particles into the carburettor of the engine. The particles were chiefly SiO_2 (74%) and Al_2O_3 (15%). The results of grain composition examination are given in Table 1.

For the purpose of abrasive wear intensity, a feeder for grinding particles was designed and made. The principle of its operation consists of pushing out (by a piston (8)) compacted grinding particles located in a thin glass tube (9) and then comminuting them by a rotating friction disc (11) in the throat (10) (Fig 1). The mandrel (7) was driven by a stepper motor (1) through a flexible coupling (2) and transmission gear composed of toothed wheels (4) and (5). Change in rotational motion of the wheels into translatory motion

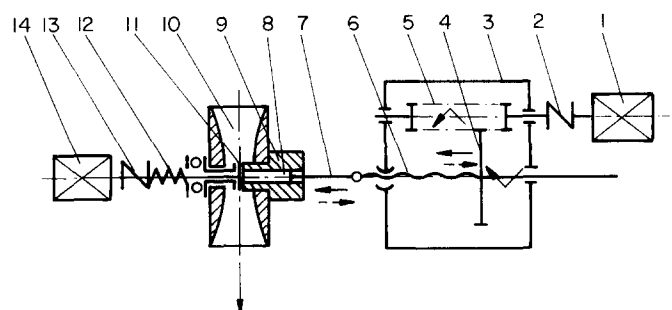


Fig 1 Kinetic diagram of the dust feeder: (1) stepped engine; (2, 13) flexible coupling; (3) frame; (4, 5) toothed wheel; (6) screw; (7) mandrel; (8) piston; (9) sleeve; (10) throat; (11) friction disc; (12) spring; (13) electric motor

of the mandrel was by a screw (6) connected to a wheel (4). The friction disc was driven by an electric motor (14) using flexible coupling (13). Its construction allows uninterrupted and uniform supply of grinding particles into an engine carburettor at a constant concentration which can be within a wide range.

The feeder for the grinding particles was located over the engine carburettor. The particles were carried from the feeder into the carburettor by a flexible duct.

To limit the wear of other elements, some changes in the lubrication system were made. These consisted of an increase in the growth of capacity of this system as well as improving the rigour of the filtration by introducing an additional 5 µm grade filter.

Eighteen four-stroke, gasoline, water cooled engines from the Polonez 1500 vehicle were tested. They were divided into six groups. The cylinders from each group had various surface topographies obtained as a result of honing by various stones attached to heads of different design. Each cylinder had a new serial set of pistons and piston rings. The pistons were made of PA12 aluminium alloy. The No 1 ring was a grey iron, chromium plated compression ring, No 2 was a grey iron, phosphate treated compression and oil ring and No 3 a grey iron oil ring. Other fundamental engine parts were unchanged during the investigation unless they became damaged or extremely worn. The cylinders were bored and honed in an engine block. The material of the cylinders of the tested engines had the following chemical constitution: 0.25% Cu, 1.98% Si, 0.7% Mn, 0.19% Cr, 0.01% Ti, 3.29% C, 0.04% S, 0.08% P. The cylinders were made of grey cast iron, the structure of which contained pearlitic matrix and graphite flakes.

Each engine with machined engine block and a set of new pistons, piston rings and piston pins was run for 30 h. It was then disassembled and measurements of the elements of the piston–piston ring–cylinder assembly were carried out. The values of cylinder wear referred to changes in their diameters, as measured with a Compact Genewa gauge at six distances from the top edge of the cylinder. Changes in the width, height, mass and clearances of the joints and the mass of the piston rings as well as the diameter of the piston coatings and the height of the piston ring grooves were also determined.

Accelerated engine wear tests under artificially increased dustiness conditions were then carried out. The engines were run under conditions of maximum effective power and maximum torque. The total duration of engine testing after running in was 21 h. The quartz particles were supplied at a rate of 1.3 g h⁻¹, which corresponds to an air dustiness of 8 mg m⁻³. After the engine tests, the dimensional and weight measurements of the fundamental engine parts were again carried out.

State of the outer layer of the tested engine cylinders

It follows from analysis of cylinder surface microgeometry after honing by various methods and with tools of different design that the surface can be fairly

precisely described using three groups of parameters: coefficients characterizing the shape of the amplitude distribution, amplitude parameters, and the mean distance between deep valleys²⁵. During the experiment the above three groups of parameters changed within the ranges used by leading engine builders.

Table 2 presents a list of confidence intervals of cylinder surface roughness parameters for separate cylinder types (the significance level was 0.95). Table 2 presents the parameters characterizing the shape of the profile amplitude distribution, R_p/R_t and R_k/R_t (according to DIN 4776), the mean space between the deep valleys OR and the amplitude parameter R_{tm} (these parameters provide the simplest description). Parameters like the so-called real oil capacity V_{oR} , deep valley width SR and depth WR were also determined. The method of OR , SR , WR and V_{oR} determination needs explanation (Fig 2).

Definition of the passage point between the region of deep valleys and the rough core region is the basis for determination of the above mentioned parameters. It was decided to determine this characteristic point (xrk , yrk) as the point of maximum curvature of the normalized bearing length curve approximated using the following function:

$$R = 0.35 [1 + (2/\pi) \arctan(A \{ \tan[(\pi/2)(2tp - 1)] - \tan[(\pi/2)(2XO - 1)] \}) + 0.3 \tan(Btp)/\tan(B)]$$

where R is roughness height, tp is bearing length ratio ($R = 0-1$), and A , XO and B are coefficients of the approximating function.

Analysis has shown that the accuracy of this approximation is very high²⁶.

The following conditions for deep valley occurrence have been assumed:

- (1) The bottom of the valley has to be placed at a depth greater than $yrk \cdot R_t$
- (2) The height of the valley has to be equal to at least 0.8 of the reduced valley depth yR , where: $yR = 2V_{oR}/(1 - xrk)$.

The shape of the valley is described by the following parameters: the mean valley height WR , i.e. the mean distance between the bottom of the valley and the closest peak projected in the direction perpendicular to the mean line, and the mean valley width – the mean distance between the adjacent peaks projected in the mean line direction (see Fig 2). The mean valley space is the mean distance between adjacent valleys.

The angle of honing for all the cylinders was 35°. The waviness parameters of the tested cylinder surfaces fell within the following ranges: $W_a = 0.13-0.25$ µm, $W_t = 0.8-2.4$ µm, $\Delta q = 0-0.1^\circ$. Measurements of the surface finish were carried out using a Talysurf 6 profilometer. Figure 3 shows the cylinder surface roughness profiles representative of all the cylinder types analysed.

From analysis of Table 2 one can find that the aim of obtaining various geometrical cylinder structures as a

Table 2 Comparison of the confidence intervals of the tested engines' cylinder surface roughness parameters

Cylinder type	Roughness parameters confidence intervals						
	R_p/R_t	R_k/R_t	$R_{tm}, \mu\text{m}$	$V_{oR}, \text{mm}^3 \text{cm}^{-2}$	$OR, \mu\text{m}$	$WR, \mu\text{m}$	$SR, \mu\text{m}$
1	0.28–0.36	0.24–0.28	6.9–8.9	0.0129–0.0185	453–543	3.6–4.4	35–41
2	0.22–0.36	0.22–0.30	2.5–4.1	0.0039–0.0113	446–606	1.7–2.3	27–39
3	0.31–0.39	0.25–0.33	4.9–9.9	0.0121–0.0167	180–244	3.5–4.5	32–38
4	0.27–0.41	0.25–0.35	2.2–4.4	0.0042–0.0098	170–236	1.1–2.3	21–39
5	0.49–0.59	0.26–0.40	4.9–7.5	0.0051–0.0089	190–254	1.9–3.5	22–30
6	0.39–0.49	0.27–0.33	2.9–4.7	0.0036–0.0086	202–268	1.2–2.4	23–37

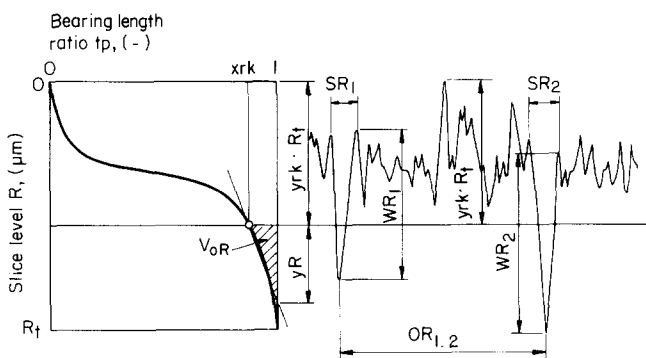


Fig 2 Method of determining the oil capacity V_{oR} and identifying deep valley as well as determining their dimensions and distribution

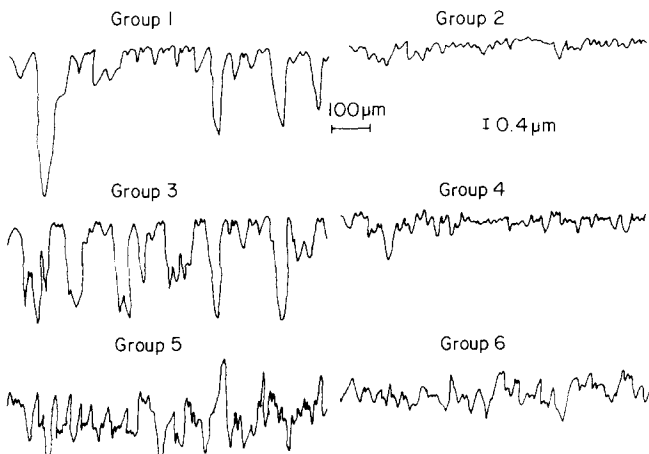


Fig 3 Examples of cylinder surface roughness profiles of different types

result of a honing process was reached. Parameters describing honed cylinder surface microgeometry changed within the limits used by leading engine builders. (R_k/R_t was kept at a relatively constant level).

Measurements of the physical properties (microhardness and residual stress) of the tested cylinder surface layer were made. Microhardness was measured on skewed polished sections with a Vicker's indenter, load 100 g, and the duration of the load was

15 s. Graphs of the microhardness distribution were not substantially different from each other. Small strain hardening of the honed cylinder surface layer was noticed.

Measurements of circumferential microstresses in the cylinder's surface layers were made by Dawidenkow's method. Successive layers of the material were removed using electrochemical etching. A solution of 60% H_3PO_4 , 20% H_2SO_4 , 20% H_2O was the electrolyte. Diagrams of the residual stresses for all the cylinders tested were similar. Compression residual stresses exist in the cylinder outer layer after honing. The maximum stresses (45–54 MPa) were at depths not exceeding 3 μm . Figure 4 shows an example of microhardness and residual stress distribution.

Counts of closed and rolled-over graphite flakes were made at a distance of 16 mm from the cylinder circumference. The values of the quotient of the number of opened flakes and the total number of flakes for all the tested cylinders were similar (0.62–0.72).

Experimental results

After the engine tests it is evident that elements operating in the extreme assemblies show the heaviest wear. A similar tendency was observed during analogous investigations²⁷. This is due to the method of supplying the grinding particles to the cylinder as well as the design of the suction manifold. Therefore the average wear values for all four cylinders and piston rings of one type were analysed. The mean values and

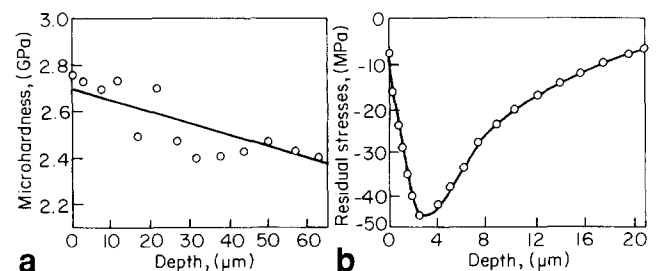


Fig 4 Diagrams of: (a) microhardness and (b) residual stress, for cylinder of type 3 after honing

Table 3 The mean values (MV) and limiting errors (LE) of the linear cylinder wear under artificially increased dustiness conditions

Cylinder type		1	2	3	4	5	6
Average cylinder wear, μm	MV	26.1	27.5	22.2	21.2	28.9	23.9
	LE	2.8	2.9	1.25	1.5	1.8	2.2
Average wear in the 'upper zone', μm	MV	33.7	35.9	29.6	29.0	41.3	32.8
	LE	3.0	3.0	2.7	2.1	3.5	1.7
Mean value of maximum cylinder wear, μm	MV	59.4	59.6	47.2	46.8	67.0	53.5
	LE	5.5	4.9	6.0	3.4	2.5	2.3

limiting errors of the measurements of wear of the cylinders and piston rings are given in Tables 3 and 4.

Table 3 presents the mean values of cylinder wear (at 10, 22, 30, 40, 75, 90 mm from the cylinder head plane, see Fig 5), the mean values of wear in the so-called 'upper zone' (only at the 10, 22, 30 mm analogous distances), and the mean values of maximum linear wear for the separate cylinders. Table 4 presents the values of piston ring wear as the average changes in width, mass and growth of clearance of the piston ring joint. Changes in piston ring height of all the tested engines were similar and amounted to: for ring No 1, 21–26 μm ; No 2, 11–14 μm ; and piston No 3, 5–7 μm . The values of piston coating wear for all the tested engines were also similar (36–42 μm). The values of wear of the piston ring groove fell within the following limits: for groove No 1, 67–74 μm ; No 2, 6–10 μm ; and groove No 3, 2–6 μm . Cylinder surface roughness R_a values after engine testing were in the range of 0.07–0.14 μm . The greatest cylinder wear

occurred near the top dead centre of the second piston ring (15–18 mm from the cylinder head plane). Figure 5 shows the typical shape of the cylinder surface in the plane perpendicular to the engine axis after the wear process.

The values of wear of the co-acting parts were very high (for example, the clearances of the piston ring joint qualified the engines for repair). However, the other engine elements did not wear too much. Engine operating parameters became worse after engine testing (mainly an increase in unitary fuel consumption took place). After engine testing, measurements of microhardness of the cylinders' surface layer in the region of the greatest wear were carried out. The microhardness of all the cylinders' surface layers was lower in comparison to the material core region (the degrees of hardening were in the ranges (–6,8)–(–15, 2%). The process of graphitization as a result of high temperatures within the cylinders is the most probable reason for this character of the microhardness distri-

Table 4 The mean values (MV) and limiting errors (LE) of the dimensional and mass wear measurements after engine operation under artificially increased dustiness conditions

Type of piston ring		Cylinder type	1	2	3	4	5	6
Average change in piston ring width, μm	1	MV	114	103	122	101	131	103
		LE	13	23	7	19	8	21
	2	MV	202	200	192	162	212	196
		LE	24	25	10	58	38	57
	3	MV	437	442	412	422	467	292
		LE	72	42	28	43	72	58
Average change in clearance of piston ring joint, mm	1	MV	0.67	0.60	0.70	0.54	0.73	0.68
		LE	0.20	0.16	0.08	0.15	0.15	0.15
	2	MV	1.20	1.19	1.13	1.08	1.26	1.17
		LE	0.13	0.08	0.13	0.13	0.10	0.30
	3	MV	2.60	2.57	2.48	2.75	2.86	2.49
		LE	0.58	0.62	0.37	0.18	0.37	0.43
Average change in piston ring mass, mg	1	MV	340	333	334	318	403	350
		LE	42	58	27	35	22	37
	2	MV	458	450	442	431	463	462
		LE	67	74	78	57	56	73
	3	MV	806	816	796	814	903	811
		LE	112	60	95	28	51	50

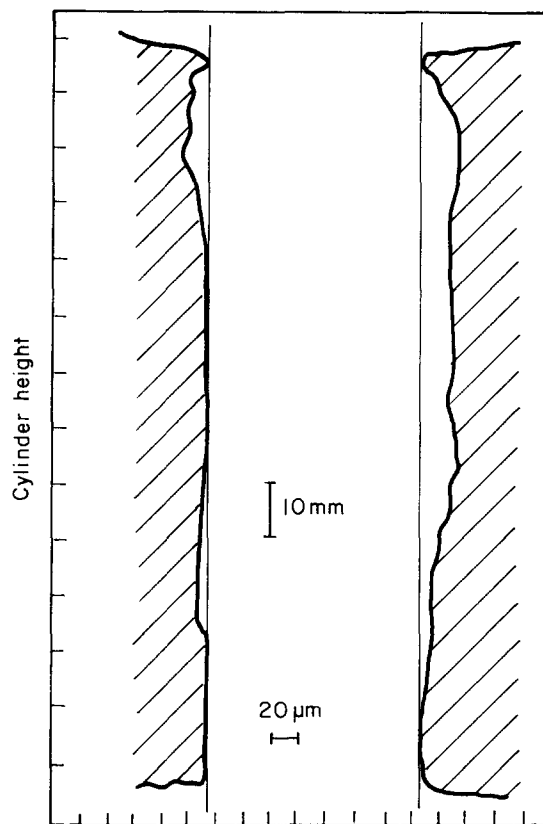


Fig 5 The shape of surface of cylinder No 4 of type 3 after engine operation under artificially increased dustiness conditions

bution. Figure 6 shows a typical microhardness distribution for a cylinder surface layer after an engine test.

Analysis of experimental results

During analysis of the effect of separate cylinder surface roughness parameters on cylinder abrasive

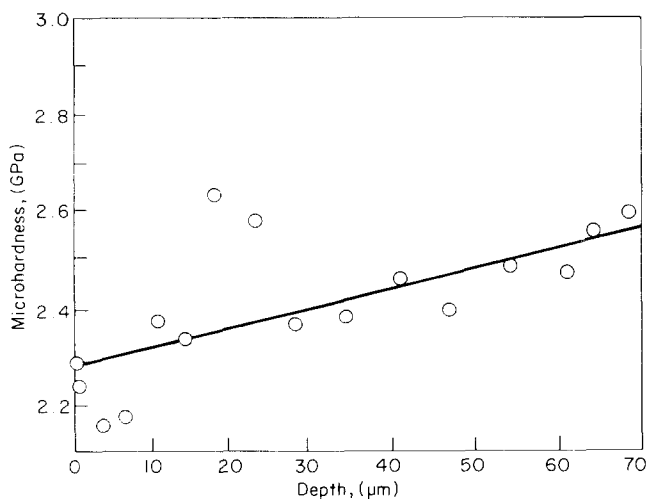


Fig 6 Microhardness distribution for cylinder No 4 of type 3 after engine operation under artificially increased dustiness conditions

wear it is necessary to compare the following types of cylinders.

Effect of the deep valleys space

At smaller roughness height ($R_{tm} = 2.2-4.4 \mu\text{m}$) and $R_p/R_t = 0.22-0.41$. Cylinders of types 2 ($OR = 450-610 \mu\text{m}$) and 4 ($OR = 170-240 \mu\text{m}$).

At greater roughness height ($R_{tm} = 4.9-9.9 \mu\text{m}$) and $R_p/R_t = 0.28-0.39$. Cylinders of types 1 ($OR = 450-540 \mu\text{m}$) and 3 ($OR = 180-244 \mu\text{m}$).

Effect of roughness height

At greater deep valleys space ($OR = 450-610 \mu\text{m}$) and $R_p/R_t = 0.22-0.36$. Cylinders of types 1 ($R_{tm} = 6.9-8.9 \mu\text{m}$) and 2 ($R_{tm} = 2.5-4.1 \mu\text{m}$).

At smaller deep valleys space ($OR = 170-240 \mu\text{m}$) and $R_p/R_t = 0.27-0.41$. Cylinders of types 3 ($R_{tm} = 4.9-9.9 \mu\text{m}$) and 4 ($R_{tm} = 2.2-4.4 \mu\text{m}$).

Effect of the shape of the amplitude distribution (the emptiness coefficients R_p/R_t)

At greater roughness height ($R_{tm} = 4.9-9.9 \mu\text{m}$) and $OR = 180-260 \mu\text{m}$. Cylinders of types 3 ($R_p/R_t = 0.31-0.39$) and 5 ($R_p/R_t = 0.49-0.59$).

At smaller roughness height ($R_{tm} = 2.2-4.7 \mu\text{m}$) and $OR = 170-270 \mu\text{m}$. Cylinders of types 4 ($R_p/R_t = 0.27-0.41$) and 6 ($R_p/R_t = 0.39-0.49$).

From an analysis of Tables 2 and 3 one can see that the initial surface roughness affects cylinder wear in the case of large wear values. Investigations under artificially increased dustiness conditions show that the deep valleys space as well as the shape of the amplitude distribution affect cylinder wear. However, a similar effect of the roughness height is small under these conditions.

There is a strong connection between the values of the R_p/R_t cylinder surface roughness coefficient and cylinder wear resistance under artificially increased dustiness. These results can be explained by the emptiness coefficient interpretation, which is a measure of linear wear of rough surfaces of the same roughness assuming identical volumetric wear. Analysis of Tables 2 and 3 shows that an increase in the deep valleys space also causes an increase in cylinder wear intensity. The possibility of abrasive particle settlement in the deep valleys may have a fundamental importance: it can reduce their injurious activity. The small influence of the cylinder surface roughness height on their abrasive wear can be explained by two opposing tendencies: the possibilities of unrestricted flow of grinding particles through the lubricating oil film in the case of smaller roughness height and larger abrasive particle settlement in the valleys in the case of larger roughness height.

The values of piston ring wear fell fundamentally within similar ranges. The piston rings belonging to the fifth engine group were an exception (particularly the compression and oil ring); the values of their wear were the largest. Generally the greatest values of cylinder wear may be the reason for the large extent of piston ring wear: extensive cylinder wear and consequently an increase in clearances and loads may have caused an increase in piston ring wear. On the

other hand, the piston rings from the fourth engine group (particularly compression and compression and oil ring) were an exception. Their amounts of wear were comparatively low. Small wear of the cylinders of these engines and their small initial roughness height were the most probable reasons for their small values of piston ring wear.

Conclusions

- (1) The influence of the microgeometry of the grey cast iron cylinders on their abrasive wear during engine operation under artificially increased dustiness conditions is substantial.
- (2) Cylinder wear during engine work under artificially increased dustiness conditions mainly depends on both the shape of the roughness profile ordinate distribution and the distance between the deep valleys after honing. The values of abrasive wear of cylinders whose surface is described by the same roughness height and similar deep valleys space is proportional to the emptiness coefficient R_p/R_t . The wear intensity of cylinders having the same surface roughness height and the shape of the profile ordinate distribution depend on the average deep valleys space OR . These cylinders wear less if their parameters OR are within the range of 170–270 μm in comparison to the cylinders for which the values of OR are 440–610 μm .
- (3) It was found that during engine operation under artificially increased dustiness conditions, the piston rings operating with cylinders with large wear intensities and high initial roughness height are the most intensively worn; however, rings operating with cylinders of lower wear intensity and small initial roughness height show the smallest wear values.

References

1. Barber C.C. and Ludema K.C. The break-in stage of cylinder-ring wear: a correlation between fired engines and a laboratory simulation. *Wear*, 1987, **118**, 57–75
2. Włodarski J. Piston internal combustion engines – tribological processes. *WKL*, Warsaw, 1982
3. Kozaczewski W. Design of the assemblies: piston-cylinder of internal combustion engines. *WKL*, Warsaw, 1979
4. Sudarshan T.S. and Bhadun S.B. Wear in cylinder liner. *Wear*, 1983, **91**, 269–277
5. Aeberli K. and Lustgarten G.A. Verbessertes Kolbenlauferhalten bei Langsamlaufenden SULZER Dieselmotoren. *Motortech. Z.* 1989, **250**, (5), 197–204
6. Grigoriew M.A. Wear resistance of the assembly: piston-cylinder of diesel engine. *Automotive Ind. (USSR)* 1985, (5), 9–12
7. Abramenko J.J. Physical chemistry of wear for cast iron cylinder liners of internal combustion engines. *Engine Build.* 1984, **3**, 38–40 (USSR)
8. Eyre T.S., Dutta K.K. and Davis F.A. Characterisation and simulation of wear occurring in the cylinder bore of the internal combustion engine. *Tribology Int.*, 1990, **23**, (1), 11–16
9. Uetz H. Einfluss der Honbearbeitung von Zylinderlaufbuchsen auf die innere Grenzschicht und den Einhaufverschleiss. *Motortech. Z.* 1969, **12**, 453–460
10. Hannoschock N. Kolbenringschmierung und -Verschleiss. *Diss. ETH* 7635, Zurich, 1985
11. Astashkevitch B.M. Wear mechanism for elements of the assembly: cylinder-piston of diesel engine. Collection of papers 'Improvement of internal combustion engine elements wear resistance' *Moskva, Machine Building*, 1972, 5–12
12. Dueck G.E. Trends in piston ring development for high output diesel engine. *SAE Paper* 851193, 1985
13. Lausch W. Gesetzmässigkeiten im Verschleiss von Zylinderlaufflächen mittelschnelleufender Viertakt-Dieselmotoren. *Motortech. Z.* 1986, **47**, (9), 329–331
14. Kleparski B. Honing process of diesel engine cylinder liners. *Silniki Spalinowe*, 1987, (3), 6–9
15. Baumgarten J. Reibung und Verschleiss am Kolbenring und Zylinderbuchsen. *Dissertation, TU Berlin*, 1968
16. Wiemann L. Die Bildung von Brandspuren auf den Laufflächen der Paarung Kolbenring-Zylinder in Verbrennungsmotoren. *Motortech. Z.* 1971, **32**, (2), 43–49
17. Duck G. Zur Laufflächengestaltung von Zylindern und Zylinderlaufbuchsen. *Motortech. Z.* 1967, **3**, 116–119
18. Day R.A., Reid T.J. and Evans D.C. Development in liner technology. *AE Technical Symposium, Paper No 28*, 1986
19. Haynes G.P., Hyde G.F., Sauter G.W. and Thornton T.E. Accelerated chromium plate piston ring wear associated with liner pitting. *SAE Paper* 831280, 1983
20. Campbell J.C. Cylinder bore surface roughness in internal combustion engines: its appreciation and control. *Wear*, 1972, **19**, 163–168
21. Stout K.J. and Spedding T.A. The characterization of the combustion engine bore. *Wear*, 1982, **83**, (2), 311–327
22. Santochi M, Vignale M. and Giusti F. A study on the functional properties of a honed surface. *CIRP Ann.* 1982, **31**, (1), 431–434
23. Dolecki, W.A., Buntow W.N., Argusow A.K., Opoczynski B.A. and Grigorjew M.A. Improvement of machine life using production engineering methods. *WNT*, Warsaw, 1983
24. Golubiev J.M., Antonov V.F. and Grebennikova F.S. Investigation of quality of the co-acting parts: cylinder-piston ring. Collection of papers: Surface quality investigations. *Zinatne, Riga*, 1976, 110–120
25. Michalski J. and Pawlus P. Parameters connected with the shape of the ordinate distribution of honed cylinders roughness profile. Proceedings of the Conference 'Metrological problems in production technology'. *Koszalin Technical University, Koszalin*, 1991
26. Michalski J. and Pawlus P. Description of the bearing length curve of the inner surface of piston engine cylinders. *Wear*, 1992, **157**, 207–214
27. Velichkin I.N., Nisnevich A.I. and Zubetova M.P. Accelerating testing of diesel engine wear resistance. *Machine Building, Moskva*, 1964